Quantification of gene expression changes in mouse disease models using a high-throughput spatial omics platform

T. AWAD, B. COOK, N. KOTOVA, I. OH, R. YIN, M. OTERO Rebus Biosystems Inc., 2255 Martin Avenue, Suite F, Santa Clara, CA.

ABSTRACT

Batch effects due to technical variability are a major problem in single cell transcriptomics. Spatial methods are no exception – their low throughput requires high numbers of technical replicates, reducing the statistical power needed to quantify differential gene expression across experimental conditions.

To overcome this problem, we took advantage of the large imaging area of the Rebus Esper spatial omics platform. We processed brain sections from three mouse genotypes in parallel - one wild type and two disease models. In addition, the Esper High Fidelity assay, based on single-molecule fluorescent in situ hybridization (smFISH), requires no amplification, yielding quantitative results with minimal batch effects. The combination of low technical variation and balanced experimental design allowed us to integrate more than 500,000 cells from multiple datasets for analysis without the need for batch correction. We were able to identify more than 12 neuronal and glial cell type clusters using 20 cell type-specific genes, and further dissect these cell types by anatomical structures utilizing the spatial information. We then performed differential gene expression of 10 disease-related genes on each cell-type subset.

These results demonstrate the ability of the Rebus Esper spatial omics platform to yield high-throughput spatial omics data with single cell resolution, low technical variation, and the sensitivity and specificity required for differential gene expression quantification.

WORKFLOW

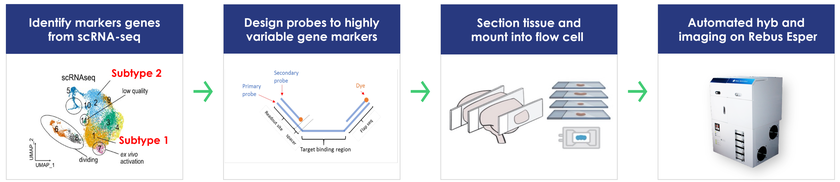

Spatial RNA Transcriptomics Workflow. Candidate cell-type specific markers are identified using unbiased scRNAseq, and a panel is designed for validation on the Rebus Esper using a high sensitivity smFISH method. Fresh-frozen tissue is sectioned and fixed onto functionalized glass coverslips, then assembled into Rebus Esper's imaging flow cell. The flow cell is installed into the Rebus Esper by connecting the cooling and reagent lines. Using automated microfluidics and high-resolution Synthetic Aperture Optics (SAO) imaging, sequential small molecule fluorescent in situ (smFISH) hybridization was performed without user intervention. The large 3cm^2 imageable area of the Rebus Esper imaging flow cell allows multiple large tissue sections to be run in parallel.

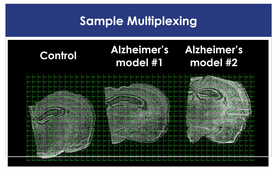

IMAGE PROCESSING AND DATA ANALYSIS

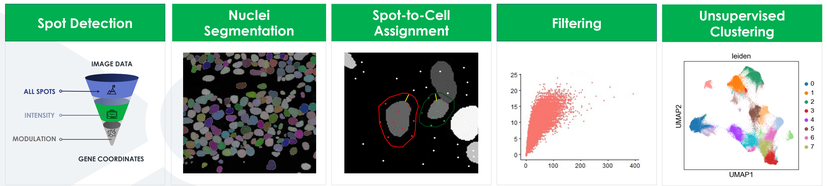

Image-based single cell expression data processing. Single transcripts of RNA were detected with customizable spot counting parameters. Nuclei were segmented using Stardist and the counts were assigned to individual cells within the nuclear boundary to minimize false-positives. The threshold for spot assignment is tunable, depending on the tissue and cell type of interest. Raw RNA and DAPI images can be further analyzed by 3rd party analysis tools.

Low run to run variability

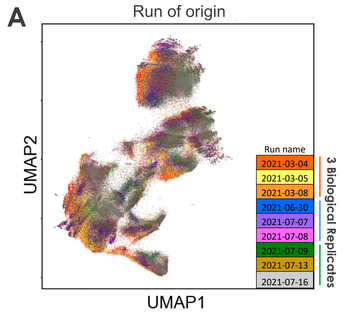

A. Run-to-run & and batch variation. UMAP plot with cells color-coded by run of origin. Total of 9 runs = 3 biological replicates x 3 technical replicates each. No batch-correction was used.

We obtained a total of 503,574 cells. After filtering low quality cells (9<n_counts<100), a total of 290,966 cells were used on this analysis.

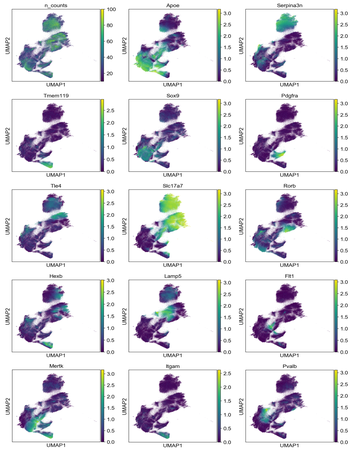

E. Expression levels of marker genes. UMAP plot showing normalized gene expression levels of 14 cell-type-specific genes. First plots corresponds to total number of transcripts per cell (n_counts).

Robust identification of main cell types

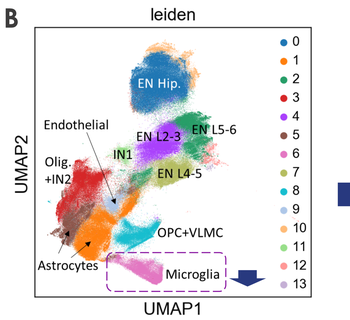

B. Unsupervised clustering & cell-type annotation. UMAP plot showing the leiden identities and annotated cell types based on expression of cell-type-specific genes. The dataset included 503,574 cells before filtering and 290,996 cells after filtering cells with 9<total-counts<100.

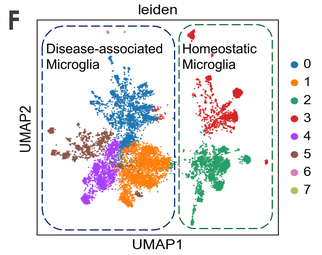

F. Clustering of Microglial cells subset. UMAP plot showing the leiden identities and microglial cell-states based on expression of disease-associated genes.

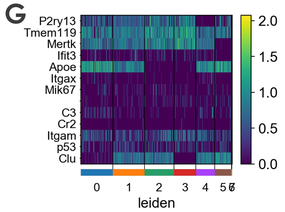

G. Heatmap showing normalized gene expression of 13 disease-related genes for microglia sub-cluster shown in fig F.

Spatial information allows further analysis of annotated cell-types

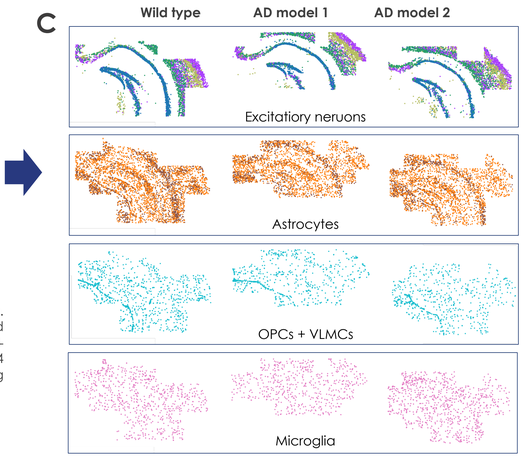

C. Spatial mapping of cell types. Individual cells, color-coded by leiden identity, plotted in the XY coordinates space. Only one of the 9 runs is shown.

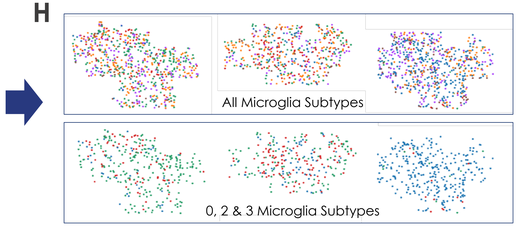

H. Spatial mapping of Microglia subtypes. Individual cells, color-coded by leiden identity, plotted in the XY coordinates space. Only one of the 9 runs is shown.

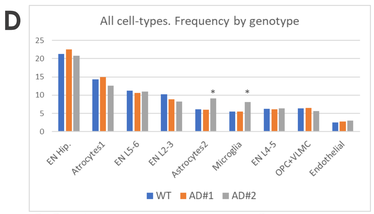

D. Relative cell-type abundance. Bar plot showing the frequency of each cell type (as percentage of total cells) in each of the three experimental conditions

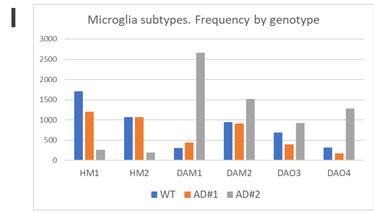

I. Relative microglia subtype abundance. Bar plot showing the frequency of each microglial subtype (as percentage of total microglia cells) in each of the three experimental conditions. (HM = homeostatic microglia, DAM = disease-associated microglia)

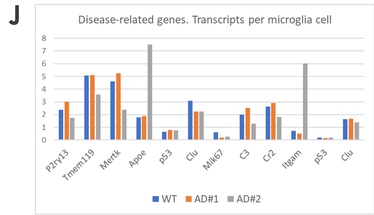

J. Expression levels of disease-associated genes. Bar-plot of raw gene expression levels of 12 disease-related genes in microglia cells.

CONCLUSIONS

- The large imageable area of the Rebus Esper platform allows sample multiplexing and balanced experimental design
- Low technical variability allows for integration of multiple datasets without batch correction steps
- The High sensitivity and specificity of the Rebus Esper High Fidelity assay enables identification of rare cell types (Microglia) and quantitative gene expression analysis